NETWORKS AND HETEROGENEOUS MEDIA
©American Institute of Mathematical Sciences
Volume **9**, Number **4**, December **2014**

doi:10.3934/nhm.2014.9.635
pp. **635–654**

MATHEMATICAL MODELLING OF A MUSHY REGION FORMATION DURING SULPHATION OF CALCIUM CARBONATE

Christos V. Nikolopoulos

Department of mathematics
University of the Aegean
Karlovasi, 83200, Samos, Greece

Abstract. The subject of the present paper is the derivation and asymptotic analysis of a mathematical model for the formation of a mushy region during sulphation of calcium carbonate. The model is derived by averaging, with the use of the multiple scales method, applied on microscopic moving - boundary problems. The latter problems describe the transformation of calcium carbonate into gypsum on the microscopic scale. The derived macroscopic model is solved numerically with the use of a finite element method. The results of some simulations and a relevant discussion are also presented.

1. **Introduction.** Corrosion of monuments is an important aspect that should be studied in relation with the conservation and restoration of cultural heritage. There are a lot of factors that cause this process and in general it is quite difficult to determine all of them together with their significance and study the problem in its full complexity. Certainly one of them is air pollution. Various pollutants existing in the atmosphere especially in big cities like Athens, Rome, etc can react, under certain conditions, with calcium carbonate and create damage, corrosion in natural building stones, marble monuments etc.

These pollutants can be sulphur dioxide (SO_2), nitrogen oxides (NO_3^-, N_2O) etc. (see [19]). One with the most importance and probably causing the most damage in stones, and therefore in monuments as well, is sulphur dioxide. The latter pollutant can react with calcium carbonate, $CaCO_3$, in the presence of water and create gypsum. The appearence of gypsum in a monument surface provides insubstantiality in a monument. Gypsum can be washed away and thus damage is done.

Therefore is of great importance if we can understand in depth this process, the factors that are involved and their importance so as to provide with a useful tool the people who work in the conservation and restoration of cultural heritage. One can proceed in this direction by deriving suitable mathematical models regarding this process.

In this paper we present such a model which accounts for the case that corrosion evolves in such a way so that gypsum and calcium carbonate coexist in a volume element of the corroded area (a type of mushy region).

2010 *Mathematics Subject Classification.* Primary: 35Q92, 35R37; Secondary: 35K57, 74G10, 74S05.

Key words and phrases. Monument corrosion, sulphation, moving boundary problems, perturbation methods, asymptotic analysis.

A model for the marble sulphation, and more specifically for the dry deposition of SO_2 in calcium carbonate stones, in the form of a macroscopic moving boundary problem, was presented initially in [5] and in [4]. Actually this model is the motivation of the present work.

Additionally a hydrodynamic model for sulfation of calcium carbonate stones in the form of a reaction diffusion system is presented and analysed extensively in [11] - [3].

In the present paper we derive a model, by modifying that of [4], which addressees the cases with an area that is partly corroded, i.e. when corroded and uncorroded parts of the material coexists in a microscale during the process. Such a model was initially introduced in [17] and extended in [18] for a similar phenomenon, the sulphation process in sewer pipes. The model introduced here is derived with the same methodology addressing the case of monument corrosion and resulting in a system of reaction diffusion equations.

The origin of the method used for the derivation of such models comes from the papers [14] and [15] which introduce macroscopic models derived from averaging microscopic free boundary problems.

Note that the multiscale approach has been also adopted to study similar processes. A very similar phenomenon as marble or calcium carbonate stones corrosion by sulphur dioxide, is concrete corrosion by sulphate. For this case, a multiscale reaction diffusion system, describing concrete corrosion, is also derived and extensively analysed in [6]-[10].

In the following parts of the paper in section 2 we proceed initially with a description of the material under study and a presentation of the actual setting of the model. Next the model equations, based on those of [5] and [4], describing the diffusion of the pollutants and the reaction causing corrosion are presented. These are assumed to account for the length scale of a pore (microstructure). With the use of multiple scales method averaging is applied to them, as in [14], [15], [17], in order to derive equations that account for the bulk of the material i.e. for a length scale related to the experimentally observed corrosion thickness. The resulting equations describe the diffusion of SO_2 and H_2O. The source term in them is related with the reaction and depends on a parameter describing, at each corresponding point of the macroscale, the evolution of the corrosion in the microscale . The latter comes from the solution of a hyperbolic equation having the form of the Eikonal equation, which in cases it has analytical solutions.

Next in section 3 a numerical approach for the solution of the resulting equations is presented. Also the Eikonal equation, describing the evolution of the corrosion inside a single pore, is solved with the use of an upwind scheme, when analytical solutions of it are not available. Various numerical simulations are also presented.

Finally a discussion of the results of this paper and possible future work extensions are given in section 4.

2. **The model.**

Marble and in general calcium carbonate stones are porous materials, composed of calcium carbonate, $CaCO_3$. In order to tackle the problem and to pose the equations describing its corrosion, we need a somehow idealized description of its microstucture. Thus initially we present briefly the basic assumptions used to describe the material, or rather an idealized version of it, that is under corrosion. Actually this is the same setting with that described also in [17], [18].

We assume that the bulk of the material under study consists of uniform cells containing calcium carbonate. To describe the porosity of the material we assume

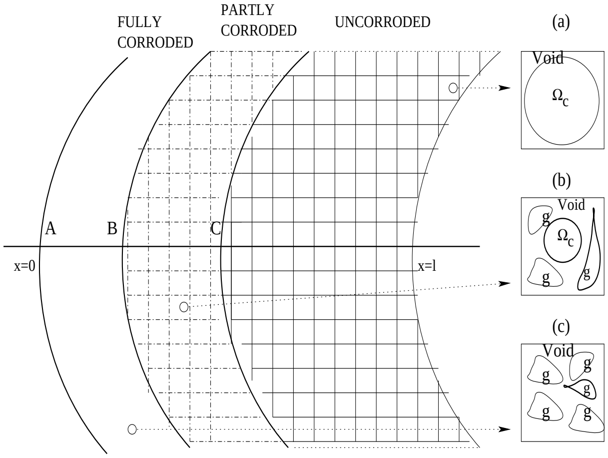

FIGURE 1. *Schematic representation of a segment of a calcium carbonate stone under corrosion. In the side cells Ω_c denotes the area of calcium carbonate and "g" denotes the gypsum segments while the rest of the cells is void.*

that the rest of the cell is void (representing the space of the pore filled with water and or air) surrounding the calcium carbonate core. Additionally we will also assume (for convenience later on in the asymptotics) that the calcium carbonate inside one cell (Ω_c in Figure 1a & b) contains also voids but of minor, very small, size so as to allow some flow inside it but no reaction taking place.

This porosity of such a calcium carbonate core, say ϕ_s, will be taken to be negligible compared to the porosity of the gypsum and that the voids inside the calcium carbonate stone have volume negligible compared with the main void of the cell ($|\Omega| - |\Omega_c|$). The reaction is taking place only in the calcium carbonate core's outer surface (in $\partial\Omega_c$ of Figure 1a & b).

Note that, summarizing the above, we assume that we have diffusion in the whole of the cell ant that the reaction takes place in the cores surface. The assumption that we have diffusion but no reaction inside the calcium carbonate core is rather unrealistic but allow us to obtain a model that it is easier to tackle analytically and especially numerically. This will be also apparent later in the asymptotic analysis that follows.

A natural and fairly simple choice is to assume that the cells of the material are cubical. Although in order to simplify our analysis, this consideration can be relaxed and assume that we have cells of square shape, and a two-dimensional geometry, as the cells, (a) to (c) shown in Figure 1 or even cells that are line segments and a one-dimensional geometry (e.g. see [17]).

More specifically in the first case we may take an infinite set of indistinguishable cubical cells, inside the material. In such a cubical cell we assume that the calcium carbonate is contained inside it forming a solid core of some shape, a cube, a sphere, or a Lamé surface, etc placed symmetrically inside the cubical cell with center that of the cell. The rest of the cell is void, filled with water and or air.

In the same way and making things simpler we may think of having cells of square shape, infinite in number, filling a plane. Again inside the cell, we have a calcium carbonate core of square, circular or elliptical, etc shape, placed symmetrically in its center. This simplification can be taken if we consider to have, in the microscopic scale, corrosion evolving in a two-dimensional way and with the square cells formed by a net of of horizontal and vertical lines that intersect in an orthogonal way. These lines may correspond to the axis of the pores (see cell (a) in Figure 1).

This can be simplified even more if we consider inside the material, long narrow cylindrical cracks which are equispaced and parallel. If we think of a vertical line intersecting the axis of these cylinders we have a sequence of line segments corresponding to calcium carbonate in the space between the voids, interchanging with line segments corresponding to these voids, i.e. the diameter of the cylindrical pores.

In each of the above three cases we may have the image inverted (this has meaning for the cubical and square cells) with now the core of the cells being the void and the rest of the cell filled with calcium carbonate. In general in the three-dimensional case we may think of a calcium carbonate grid filling the space.

Such a material may be corroded due to the penetration of sulphur dioxide inside the pores causing a reaction which transforms calcium carbonate into gypsum. The basic reaction describing the fact that SO_2 reacts with calcium carbonate CaCO_3 forming gypsum $\mathrm{CaSO}_4 \cdot 2\mathrm{H}_2\mathrm{O}$ and causing the corrosion of the monument, is the following:

$$\mathrm{CaCO}_3 + \mathrm{SO}_2 + \frac{1}{2}\mathrm{O}_2 + 2\mathrm{H}_2\mathrm{O} \xrightarrow{\mathrm{k_u}} \mathrm{CaSO}_4 \cdot 2\mathrm{H}_2\mathrm{O} + \mathrm{CO}_2. \tag{1}$$

More specifically we have that one mole of calcium carbonate reacts with one mole of sulphur dioxide and two moles of water to produce one mole of calcium sulfate dihydrate, i.e. gypsum, and one of carbon dioxide. For the reaction to take place we must have a film of water or water droplets covering the calcium carbonate inside the pores. Then the presence of water together with that of SO_2, diffused inside the pores of the marble or of the calcium carbonate stone, since it exist as a pollutant in the atmospheric air, triggers the reaction forming gypsum. An external layer of gypsum is formed which may be drained out or form crust and then exfoliate.

This is the reaction that accounts for the dry deposition of SO_2 on calcium carbonate stones (see [4]) and it is the most usual process causing damage in stones.

We consider a model for gypsum formation which allows gypsum and calcium carbonate to coexist at some volume element. This element may be specified as one cell as those already described, containing a single pore, or in general as one having its length side of order similar to the radius of a cross-section of a typical pore.

More specifically we have that through the calcium carbonate and due to its porosity and the cracks existing in it, there is diffusion (dispersion) of SO_2 which in the presence of water (needed for the reaction) reacts with the calcium carbonate, forming gypsum. The reaction takes place initially at the cracks' inner surface surrounding the pure solid calcium carbonate. Then gypsum is formed, having larger porosity than the marble and thus new cracks are formed and diffusion takes place in the gypsum - void (containing no solid and filled with air and water) due to cracks area.

Such a situation is represented by the cell (b) in Figure 1 where a single cell is partly corroded and then in the cell (c) in Figure 1 where the cell is fully corroded and the transformation to gypsum is now complete. As the process evolves, in a planar way as it is assumed in Figure 1, there are cells not corroded yet, right to the point point C, partly corroded, between the points B and C, and fully corroded between the points A and B. In case that the points B and C coincide then we have a sharp interface of the corrosion front, the case studied in [5], [4], while if this does not occur we have a type of mushy region formed which is the case addressed here.

In order to model this phenomenon and to be able to apply the homogenization process we may study initially the above process as taking place in one single pore, or rather cell, and then with the use of the multiple scales method we derive equations for the whole of the material.

Finally due to the fact that the porosity of the gypsum is larger than that of the calcium carbonate, as gypsum is formed and calcium carbonate is consumed we have expansion of the overall volume of the material (see [5]). To keep things simple, as in [17], [18], we assume in the following that this volume expansion is negligible, compared with the length scale of the corroded layer of the material.

The model equations. We assume that SO_2 diffuses inside the voids of the material and its concentration satisfies the equation

$$u_t = D_s \Delta u, \tag{2}$$

where u is the molar concentration of SO_2, D_s is diffusivity of SO_2 in the voids of the pores. Moreover $u = u(x,t)$ and in general $x \in \mathbb{R}^n$, $n = 1, 2, 3$ depending the macroscopic geometry of the material under consideration. In general we assume that $x \in \Omega_M$, where Ω_M is the domain of the material under study.

The boundary conditions at the interface Γ_M of the corroded - uncorroded material must account for the fact that we have motion of the boundary Γ_M due to the transformation of calcium carbonate to gypsum and that this motion should be related to the rate of the reaction. The latter can be specified by a direct application of the law of mass action (see [19]). For w being the molar concentration of the water and C_c that of calcium carbonate, the rate of the reaction according to equation (1) will be

$$k_u C_c \, u \, w^2.$$

For C_c constant we set $k = k_u C_c$. However according to [4] we need to take into account the fact that when the concentration of the water w is smaller than a threshold w_l then the reaction does not takes place at all, while it gains its full speed when w is larger than an upper threshold w_u. We have that when $w_l < w < w_u$ the reaction does not attain its full speed and this is due to the fact that the $CaCO_3$ is not coated by a continuous film but more likely coated by humid spots. Therefore in order to address that behaviour we express the rate of reaction as

$$g(w) k \, u \, w^2,$$

where $g(w) = \frac{\min(\max(w, w_l), w_u) - w_l}{w_u - w_l}$, so that $g(w) = 0$ for $w \le w_l$ and $g(w_u) = 1$ for $w \ge w_u$ while it increases linearly between w_l and w_u. Reasonable values for these thresholds (see [4]) are $w_l = 0.25$ and $w_u = 0.75$.

Note that in [4] the process is separated in two regimes and that the reaction rate can grow to infinity giving $u = 0$ in the boundary and a sharp interface. In our case we want to avoid this since we want to focus in those cases that we do not have a purely diffusive front in the macroscale but rather an area, a mushy region, that gypsum and calcium carbonate coexists for some period of time. Thus we proceed with the above approach by taking at all times that the reaction rate has the form given by the law of mass action.

In accordance with the above we expect that at the boundary separating calcium carbonate and gypsum Γ_M (consisted by the union of these boundaries in the cells of the material), the kinetic condition should have the form "speed of the boundary $\times$ calcium carbonate concentration $\propto$ rate of reaction", i.e.

$$C_c\, v = g(w) k\, u\, w^2, \quad x \in \Gamma_M, \tag{3}$$

where $v = v(x,t)$ is the speed of the moving boundary Γ_M.

In addition the flux of u arriving at the interface is expected to be consumed by the chemical reaction transforming calcium carbonate into gypsum and therefore we have

$$-D_s \left.\frac{\partial u}{\partial n}\right|_J = C_c v + uv, \quad x \in \Gamma_M, \tag{4}$$

where n is the outward normal vector at a point of the moving boundary Γ_M, and $u_n|_J := u_n^+ - u_n^-$ denotes the jump of the flux at the boundary. Equation (4) expresses the total molar balance of SO_2 (see [4]). The first term "$C_c v$" includes the loss rate due to the reaction while the second one "uv" stands for the advective flux due to the transport of the residual SO_2. Given that $v = g(w)k_u uw^2$ we get

$$-D_s \left.\frac{\partial u}{\partial n}\right|_J = g(w)k_u C_c uw^2 + g(w)k_u u^2 w^2 = g(w)k_u uw^2(C_c + u), \quad x \in \Gamma_M.$$

Note that assuming that the transport of the residual SO_2 is negligible we have just $-D_s \left.\frac{\partial u}{\partial n}\right|_J = g(w)k_u C_c uw^2$.

The diffusion process for the water molar concentration w can be described by similar equations. Water is diffused inside the pores of the material, that is

$$w_t = D_w \Delta w, \tag{5}$$

where D_w is diffusivity of H_2O in the voids of the pores.

The flux of w arriving at the interface similarly is expected to be consumed by the chemical reaction while the residual water is transferred with a rate proportional to the boundary speed. Hence we have

$$-D_w \left.\frac{\partial w}{\partial n}\right|_J = 2C_c v + wv, \quad x \in \Gamma_M, \tag{6}$$

or

$$-D_w \left.\frac{\partial w}{\partial n}\right|_J = 2g(w)k_u C_c uw^2 + g(w)k_u uw^3 = g(w)k_u uw^2(2C_c + w), x \in \Gamma_M. \tag{7}$$

Scaling. The equations for u and w can be scaled to obtain a dimensionless form.

We scale x with l, and the dimensionless length y is given by $y = \frac{x}{l}$ where l is a typical length of the observed corrosion in a period of years i.e. an empirical estimation of the corrosion length in such a time period or a macroscopic length associated with the thickness of the calcium carbonate stone.

We scale u, w with λ_1, λ_2 (atmospheric concentrations), respectively. We take λ_1 to be a typical molar concentration of SO_2 in the ambient atmosphere. Also λ_2 is similarly a typical concentration of the humidity. Given that in the ambient atmosphere we have variation of these concentrations during the period of one or more years or even daily we can take the average values of them during a simulation period as typical. We set $U = \frac{u}{\lambda_1}$, $W = \frac{w}{\lambda_2}$, for U and W the dimensionless concentrations of SO_2 and H_2O respectively. Additionally the speed of the boundary should be scaled with the quantity l/t_0, i.e. $v = \mathsf{V}\, l/t_0$ where t_0 is a time scale chosen appropriately so as to balance the terms in the kinetic condition. The latter means that we must choose $t_0 = \frac{l}{k_u\,\lambda_1\,\lambda_2^2}$ and we set $\tau = t/t_0$ for τ the dimensionless time. The resulting dimensionless equations have the form

$$\epsilon_1 \frac{\partial U}{\partial \tau} = \Delta U, \quad \text{in the voids,} \tag{8a}$$

$$\mathsf{V} = g(W) U\, W^2, \quad \text{on} \quad \Gamma_M, \tag{8b}$$

$$\gamma_1 \left. \frac{\partial U}{\partial n} \right|_J + g(W) U\, W^2\, (1 + \beta_1 U) = 0, \quad \text{on} \quad \Gamma_M, \tag{8c}$$

$$\epsilon_2 \frac{\partial W}{\partial \tau} = \Delta W, \quad \text{in the voids,} \tag{8d}$$

$$\gamma_2 \left. \frac{\partial W}{\partial n} \right|_J + g(w) U\, W^2 (2 + \beta_2 W) = 0, \quad \text{on} \quad \Gamma_M, \tag{8e}$$

for $U = U(y, \tau)$, $W = W(y, \tau)$. Regarding the dimensionless parameters appearing in the equations we have $\epsilon_1 = \frac{l^2}{t_0 D_s} = \frac{l k_u \lambda_1 \lambda_2^2}{D_s}$, $\gamma_1 = \frac{D_s}{l k_u C_c \lambda_2^2}$, $\beta_1 = \frac{\lambda_1}{C_c}$, $\epsilon_2 = \frac{l^2}{t_0 D_w} = \frac{D_s}{D_w} \frac{l k_u \lambda_1 \lambda_2^2}{D_s}$, $\gamma_2 = \frac{D_w}{l k_u C_c \lambda_1 \lambda_2}$, $\beta_2 = \frac{\lambda_2}{C_c}$. Note also that $\epsilon_1 = \frac{1}{\gamma_1} \frac{\lambda_1}{C_c}$, $\epsilon_2 = \frac{D_s}{D_w} \epsilon_1$, $\gamma_2 = \frac{1}{\epsilon_2} \frac{\lambda_2}{C_c}$.

Also we assume that length scales are chosen so as to have $\gamma_1 = \gamma_u \frac{1}{\delta}$, $\gamma_2 = \gamma_w \frac{1}{\delta}$ for $\gamma_u = \gamma_w = O(1)$ where δ is the ratio of the macroscopic and microscopic length scales that is specified in detail later. We need this so as to be able to balance the terms of the kinetic condition and be able to capture the motion of the boundary in the microscopic scale. This will be apparent later in equation(18) (see also [17], [18]).

Since we have assumed that the material consists of identical cells, we can focus our study on the behaviour of these equations in a single cell.

We consider a line segment, square or a cubic cell, say Ω, with boundary $\partial\Omega = \Gamma_e$, which initially contains pure calcium carbonate occupying the domain Ω_c with its boundary $\partial\Omega_c = \Gamma_c$ separating it initially from the void space. Namely we take the void, inside the cell, to be specified by the boundaries Γ_e and Γ_c and its domain before the corrosion process starts is $\Omega_v = \Omega \setminus \Omega_c$. The minor voids inside Ω_c due to their negligible size, as assumed previously, are not taken into account. The area of Ω_v should be such that $\frac{|\Omega_v|}{|\Omega|} = \phi_c$ for ϕ_c being the porosity of the calcium carbonate (see Figure 1 at (a)). As corrosion evolves and gypsum is formed the boundary Γ_c now separates pure calcium carbonate from the gypsum and void parts of the rest of the element. We denote the gypsum-void part of the element by Ω_g and we have $\Omega = \Omega_g \cup \Omega_c$ (see Figure 1 at (b)). Note that at $t = 0$, $\Omega_g(0) = \Omega_v$. This process continues until the transformation of the calcium carbonate to gypsum is completed and have $\Omega = \Omega_g$, $\Gamma_c = \emptyset$ (see Figure 1 at (c)) .

Note that we can take Ω_M as the infinite union of identical cells Ω. Similarly the interface between calcium carbonate and gypsum-void segments Γ_M can be seen as the infinite union of the boundaries Γ_c in each cell. Also for convenience for the rest of the presentation we may think of the cell as being a square one, unless it is stated otherwise.

Additionally to the equations expressing the diffusion of SO_2 and of H_2O on a single cell and the reaction in the interface of gypsum and calcium carbonate we need to pose conditions in the fixed boundary of the cell.

More precisely, on the cell boundary, Γ_e, periodic conditions should be applied for the variable U. This is due to the fact that we have an infinite set of identical cells inside the material. These periodic conditions can be summarized, according to [17], [14], in the following form :

$$n \cdot \nabla U|_{\partial\Omega} = 0 \quad x \in \Gamma_e. \tag{9}$$

Finally periodic conditions for w can be summarized as well in the equation,

$$n \cdot \nabla W_{\partial\Omega} = 0 \quad x \in \Gamma_e. \tag{10}$$

Therefore summarizing the above we have that in one cell of the material the following equations for U and W hold

$$\epsilon_1 \frac{\partial U}{\partial \tau} = \Delta U, \quad x \in \Omega_v, \tag{11a}$$

$$\mathsf{V} = g(W)U\,W^2, \quad x \in \Gamma_c, \tag{11b}$$

$$\gamma_1 \left.\frac{\partial U}{\partial n}\right|_J + g(W)U\,W^2(1+\beta_1 U) = 0, \quad x \in \Gamma_c, \tag{11c}$$

$$n \cdot \nabla U_{\partial\Omega} = 0 \quad x \in \Gamma_e, \tag{11d}$$

$$\epsilon_2 \frac{\partial W}{\partial \tau} = \Delta W, \quad x \in \Omega_v, \tag{11e}$$

$$\gamma_2 \left.\frac{\partial W}{\partial n}\right|_J + g(W)U\,W^2(2+\beta_2 W) = 0, \quad x \in \Gamma_c, \tag{11f}$$

$$n \cdot \nabla W_{\partial\Omega} = 0 \quad x \in \Gamma_e. \tag{11g}$$

Rescaling and averaging. In the following we apply the methodology described in [14], [15] and also in [17], [18]. This method can be relatively easily adapted to our case together with the necessary modifications and it is presented here for completeness..

We consider two spatial scales for the problem, the macroscopic length scale represented by the variable y and a microscopic length scale represented by the variable z.

Let d be a microscopic length scale. The length scale d can be taken to be of order of an average distance between two neighbouring voids inside the material or the average diameter of a void inside a specified cell. This distance can be used as a characteristic length in the microscopic scale. We expect that $d \ll l$, for l the macroscopic length scale, and their ratio is $\delta = \frac{d}{l} \ll 1$. More specifically we have that for x being the dimensional original distance, $x = ly$ and $x = dz$ with $\delta = \frac{d}{l} \ll 1$.

In addition for the following analysis to hold we will assume that even for the case that we have $\epsilon_{1,2} \ll 1$ the condition $1 \gg \epsilon_{1,2} \gg \delta$ holds.

As a next step, we take

$$U = U(y, z, \tau), \quad W = W(y, z, \tau).$$

The multiple scales approach (see [13]) gives instead for the spatial derivative $\nabla_y U$ at the point (y, z, t) the expression

$$\nabla_y U + \frac{1}{\delta}\nabla_z U.$$

Also the boundary Γ_c can be described by some function $\mathsf{s} = \mathsf{s}(y, \tau)$ ($\mathsf{s} = s/l$ for s the dimensional position of the boundary) giving the position of the boundary at each time. The position of the boundary s can be also rescaled with d and we take $S = \frac{s}{d}$ $(= \frac{l}{d}\mathsf{s} = \frac{1}{\delta}\mathsf{s})$.

Rescaling also with d the speed of the boundary V, will give $\mathsf{V} = \delta\mathcal{V}$, where $\mathcal{V}$ is the new dimensionless variable for the speed ($v = \mathsf{V}\, l/t_0 = \mathcal{V}\, d/t_0$, or $\mathsf{V} = \delta\mathcal{V}$). This implies that $\mathcal{V} = g(W)UW^2$ on Γ_c.

If we denote by $\mathcal{S}$ the function representing the position of the boundary in the form $\mathcal{S}(y,z,\tau) = 0$, ($\mathcal{S}(y,z,\tau) = z_2 - S(y,z_1,\tau) = 0$), we have that the rescaled speed of the boundary $\mathcal{V}$, has the form

$$\mathcal{V} = \frac{\partial\mathcal{S}}{\partial\tau}\frac{1}{|\nabla_z\mathcal{S} + \delta\nabla_y\mathcal{S}|}.$$

Initially we focus in the equation for U. Application of the multiple scales method implies

$$\epsilon_1 U_\tau = \frac{1}{\delta^2}\nabla_z^2 U + \frac{2}{\delta}\nabla_y\nabla_z U + \nabla_y^2 U.$$

Regarding the condition(4), we have

$$\delta\mathcal{V}\,(1+\beta_1 U) = \delta\frac{\partial\mathcal{S}}{\partial\tau}\frac{1}{|\nabla_z\mathcal{S} + \delta\nabla_y\mathcal{S}|}\,(1+\beta_1 U) = -\gamma_u\frac{1}{\delta}\,n\cdot\,[\nabla_z U + \delta\nabla_y U]|_J\,,$$

and also at the same boundary

$$\gamma_u\, n\cdot\,[\nabla_z U + \delta\nabla_y U]|_J + \delta^2 g(W)UW^2(1+\beta_1 U) = 0.$$

At the boundary Γ_e similarly we have

$$n\cdot[\nabla_z U + \delta\nabla_y U] = 0. \tag{12}$$

In the following we proceed with a formal asymptotic expansion for U, W and S.

The equation for U, by assuming that $U \sim U_0 + \delta U_1 + \ldots$, $W \sim W_0 + \delta W_1 + \ldots$ takes the form

$$\begin{aligned}\epsilon_1 U_{0\tau} + \delta\epsilon_1 U_{1\tau} + \delta^2\epsilon_1 U_{2\tau} + \ldots \quad = \quad & \frac{1}{\delta^2}\nabla_z^2 U_0 + \frac{2}{\delta}\nabla_z\nabla_y U_0 + \nabla_y^2 U_0 \\ & + \frac{1}{\delta}\nabla_z^2 U_1 + 2\nabla_z\nabla_y U_1 + \delta\nabla_y^2 U_1 \\ & + \nabla_z^2 U_2 + 2\delta\nabla_z\nabla_y U_2 + \delta^2\nabla_y^2 U_2 \\ & + \delta\nabla_z^2 U_3 + 2\delta^2\nabla_z\nabla_y U_3 + \ldots.\end{aligned}$$

At the points (y,z,τ) of the boundary Γ_c, we have for $\mathcal{S} = \mathcal{S}_0 + \delta\mathcal{S}_1 + \ldots$, and $|\nabla_z\mathcal{S} + \delta\nabla_y\mathcal{S}| = |\nabla_z\mathcal{S}_0 + \delta\nabla_y\mathcal{S}_0 + \delta\nabla_z\mathcal{S}_1 + \ldots|$, that

$$\frac{\partial\mathcal{S}_0}{\partial\tau}\frac{1}{|\nabla_z\mathcal{S}_0|}\,(1+\beta_1 U_0) = -\gamma_u\, n\cdot\left[\frac{1}{\delta^2}\nabla_z U_0 + \frac{1}{\delta}\nabla_y U_0 + \frac{1}{\delta}\nabla_z U_1 + \nabla_y U_1 + \nabla_z U_2 + \ldots\right]\Bigg|_J,$$

$$g(W_0)U_0W_0^2(1+\beta_1 U_0) + \gamma_u\, n\cdot\left[\frac{1}{\delta^2}\nabla_z U_0 + \frac{1}{\delta}\nabla_y U_0 + \frac{1}{\delta}\nabla_z U_1 + \nabla_y U_1 + \nabla_z U_2\right]\Bigg|_J + \ldots = 0.$$

Similarly at the points (y,z,τ) of the boundary Γ_e we have

$$n\cdot\left[\frac{1}{\delta^2}\nabla_z U_0 + \frac{1}{\delta}\nabla_y U_0 + \frac{1}{\delta}\nabla_z U_1 + \nabla_y U_1 + \nabla_z U_2\right] + \ldots = 0 \tag{14}$$

For order $O(\frac{1}{\delta^2})$ terms we have $\nabla_z^2 U_0 = 0$ in Ω_g, $n\cdot\nabla_z U_0 = 0$ in Γ_c, i.e. at $z = S$ and $n\cdot\nabla_z U_0 = 0$ in Γ_e. From these equations and a direct application of the maximum principle we deduce that $U_0 = U_0(y,\tau)$.

For order $O(\frac{1}{\delta})$ terms we have that $2\nabla_z\nabla_y U_0 + \nabla_z^2 U_1 = \nabla_z^2 U_1 = 0$, in Ω_g, $n \cdot [\nabla_y U_0 + \nabla_z U_1]|_J = 0$ on Γ_c and $n \cdot [\nabla_y U_0 + \nabla_z U_1] = 0$ on Γ_e. Due to the fact that $U_0 = U_0(y,\tau)$ and that $n \cdot \nabla_y U_0|_J = 0$. we have similarly $U_1 = U_1(y,\tau)$.

Note that these set of equations for $O(\frac{1}{\delta})$ and $O(\frac{1}{\delta^2})$ are exactly the same as in [14]. Having not allowing diffusion inside the calcium carbonate core of a single cell would give for $O(\frac{1}{\delta})$ terms $n \cdot \nabla_z U_1 = -n \cdot \nabla_y U_0$ leading to dependence on z of U_1. Consequently we would obtain an extra term in the macroscopic equation later on, expressing the fact that diffusion takes place not in a whole square cell but in an evolving part of it. More precisely we will have the effect of changing effective diffusivity, depending in $\Omega_c(y,\tau)$, in the derived macroscopic diffusion equations. To avoid further analytical and numerical complications such a situation is avoided here by allowing flow inside the calcium carbonate core of the cell due to very small pores existing in it.

Next for $O(1)$ terms, we have

$$\epsilon_1 U_{0\tau} = \nabla_y^2 U_0 + \nabla_z^2 U_2, \tag{15}$$

while at the boundary Γ_c,

$$\frac{\partial \mathcal{S}_0}{\partial \tau}\frac{1}{|\nabla_z \mathcal{S}_0|}(1+\beta_1 U_0) = -\gamma_u\, n \cdot [\nabla_y U_1 + \nabla_z U_2] = g(W_0)U_0\, W_0^2(1+\beta_1 U_0). \tag{16}$$

We next proceed by averaging the field equation, (15). In this way eliminate the z-dependence from the equations and obtain a model depending only in y and τ, describing the phenomenon at the macroscopic scale. This can be done by integrating both sides of the equation with respect to z over the cell area, Ω. Note that $A(y,\tau) = \int_{\Omega_g} dz$ and given that the area of voids inside the cell is $\phi_g A(y,\tau) + \phi_s \int_{\Omega_c} dz \simeq \phi_g A(y,\tau)$, for $\phi_s \ll \phi_g < 1$, we have that

$$\int_{\Omega_g} \left[\epsilon_1 U_{0\tau} - \nabla_y^2 U_0\right] dz = \int_{\Omega_g} \nabla_z^2 U_2 dz = \int_{\Gamma_c \cup \Gamma_e} n \cdot \nabla_z U_2 dz,$$

or

$$\phi_g A(y,\tau)\left[\epsilon_1 U_{0\tau} - \nabla_y^2 U_0\right] = \int_{\Gamma_c} n \cdot \nabla_z U_2 dz + \int_{\Gamma_e} n \cdot \nabla_z U_2 dz.$$

In addition we have $\int_{\Gamma_c \cup \Gamma_e} n \cdot \nabla_y U_1 dz = 0$. Also the symmetry conditions at the cell boundary Γ_e give $\int_{\Gamma_e} n \cdot \nabla_z U_2 dz = 0$ and moreover we have that $\int_{\Gamma_c \bigcap \Gamma_e} n \cdot \nabla_z U_2 dz = 0$.

Therefore the source term $F_u := \int_{\Gamma_c} n \cdot \nabla_z U_2 dz + \int_{\Gamma_e} n \cdot \nabla_z U_2 dz$, due to the expansion of the Stefan and the Robin conditions at the boundary Γ_c, takes the form

$$F_u(U_0,W_0) := \int_{\Gamma_c \setminus (\Gamma_c \bigcap \Gamma_e)} n \cdot \nabla_z U_2 dz = -\frac{1}{\gamma_u} g(W_0)U_0 W_0^2(1+\beta_1 U_0)\int_{\Gamma_s} dz,$$

for $\Gamma_s = \Gamma_c \setminus (\Gamma_c \bigcap \Gamma_e)$. We also write $L := \int_{\Gamma_s} dz$ the length of Γ_s appearing in the expression for $F_u(U_0,W_0)$.

On summarizing, the final set of equations that are derived by this process is

$$\epsilon_1 U_{0\tau} - \nabla_y^2 U_0 = -\frac{1}{\gamma_u \phi_g} g(W_0)U_0 W_0^2(1+\beta_1 U_0)\frac{L(y,\tau)}{A(y,\tau)}, \tag{17}$$

$$\frac{\partial \mathcal{S}_0}{\partial \tau}\frac{1}{|\nabla_z \mathcal{S}_0|} = g(W_0)U_0 W_0^2 \quad \text{on} \quad \Gamma_c. \tag{18}$$

In exactly the same way averaging process can be applied in the equation for W and we obtain

$$\epsilon_2 W_{0\tau} - \nabla_y^2 W_0 = -\frac{1}{\gamma_w \phi_g} g(W_0) U_0 W_0^2 (2 + \beta_2 W_0) \frac{L(y,\tau)}{A(y,\tau)}. \tag{19}$$

By the fact that to first order terms we have $\mathcal{S} = z_2 - S(y, z_1, \tau) \simeq \mathcal{S}_0$, we get for a square cell $\Omega = [-1,1] \times [-1,1]$,

$$L(y,\tau) = \textstyle\int_{\Gamma_s} dz = 4 \int_0^1 \sqrt{1 + \left(\frac{\partial S}{\partial z_1}\right)^2} dz_1.$$

$$A(y,\tau) = 4 \left[1 - \textstyle\int_0^1 S(y, z_1, \tau) dz_1\right].$$

The factor 4 in the above relations comes from the fact that due to symmetry, assumed here, it is enough to specify S in $[0,1] \times [0,1]$.

The derived equations account for the actual concentrations of U and W of SO_2 and H_2O, while the effective concentrations $\bar{U}$ and $\bar{W}$ are given by the relations $\bar{U} = \phi U$ and $\bar{W} = \phi W$ respectively. Here $\phi = \phi(y,\tau)$ is the porosity of the material $\phi_c \leq \phi := (\phi_g - \phi_c) \frac{A(y,\tau) - A(y,0)}{(4 - A(y,0))} + \phi_c \leq \phi_g$. We may now consider the macroscale domain Ω_M in which the equations for U and W apply. A natural choice for boundary conditions to be taken is Dirichlet conditions in the form, e.g. for U, $\bar{U} = \phi U = c(t)$. This function $c(t)$ may account for the variations of SO_2 in the ambient atmosphere. For convenience and simplicity we may use a constant average value of SO_2 at the boundary and set $c(t) = \lambda_1$. Thus we take, after appropriate scalling, $\phi U = 1$ on $\partial\Omega_M$.

For cases that we have a planar propagation of the corrosion regime we can take the problem to be one-dimensional. Also symmetry conditions may be imposed at the center, say at $x = l$, of the material under study while, $y \in \mathbb{R}$ and $0 < y < 1$ ($\Omega_M = [0,1]$). Therefore a possible set of boundary condition for the problem can be

$$\phi(0,\tau) U(0,\tau) = 1, \quad \frac{\partial(\phi U)}{\partial y}(1,\tau) = 0. \tag{20}$$

Summarizing, the equations derived, for the case that we consider one dimension in the macroscale, and by dropping the subscripts in the notation for U, W and $\mathcal{S}$ since $U \simeq U_0$ $W \simeq W_0$, $\mathcal{S} \simeq \mathcal{S}_0$, we have

$$\epsilon_1 U_\tau - U_{yy} = -\frac{1}{\gamma_u \phi_g} g(W) U W^2 (1 + \beta_1 U) \frac{L(y,\tau)}{A(y,\tau)}, \quad 0 < y < 1, \quad \tau \geq 0, \tag{21a}$$

$$U(0,\tau) = \frac{1}{\phi(0,\tau)}, \quad U_y(1,\tau) + \frac{\phi_y(1,\tau)}{\phi(1,\tau)} U(1,\tau) = 0, \tag{21b}$$

$$U(y,0) = U_a(y), \tag{21c}$$

$$\epsilon_2 W_\tau - W_{yy} = -\frac{1}{\gamma_w \phi_g} g(W) U W^2 (2 + \beta_2 W) \frac{L(y,\tau)}{A(y,\tau)}, \quad 0 < y < 1, \quad \tau \geq 0 \tag{21d}$$

$$W(0,\tau) = \frac{1}{\phi(0,\tau)}, \quad W_y(1,\tau) + \frac{\phi_y(1,\tau)}{\phi(1,\tau)} W(1,\tau) = 0, \tag{21e}$$

$$W(y,0) = W_a(y), \tag{21f}$$

$$-\frac{\partial S}{\partial \tau} \frac{1}{\sqrt{1 + \left(\frac{\partial S}{\partial z_1}\right)^2}} = g\left(W(y,\tau)\right) U(y,\tau) W^2(y,\tau), \quad 0 < z_1 < 1, \quad \tau \geq 0, \tag{21g}$$

$$S(y,z_1,0)=S_a(z_1),\quad \frac{\partial S}{\partial z_1}(y,0,\tau)=0, \tag{21h}$$

$$\phi(y,\tau)=(\phi_g-\phi_c)\frac{A(y,\tau)-A(y,0)}{(4-A(y,0))}+\phi_c, \tag{21i}$$

$$L(y,\tau)=4\int_{S(y,z_1,\tau)}dz_{\Gamma_s},\quad A(y,\tau)=4\left[1-\int_0^1 S(y,z_1,\tau)dz_1\right]. \tag{21j}$$

Here U_a and W_a are the initial conditions for U and W respectively and a natural choice to make is to take $U_a=W_a=0$. Also S_a is the initial position of the moving boundary Γ_c, applied to all the cells inside the material, assumed to be independent of y, while for $\tau>0$ its position is given by the points (z_1,z_2) for which we have $z_2=S(y,z_1,\tau)$.

In general, also having in mind the results in [17], [18], we can deduce that if the motion of the boundary is driven by a reaction in such a process the above method results in a macroscopic diffusion equation with a source term having the form : "rate of the reaction × length of the moving boundary in a cell / Area of gypsum-void in the cell". The corrosion state of a single cell, expressed by the quantities A and L, represents the state of corrosion at each corresponding macroscopic point y. In this way the information of the corrosion evolution in the microscopic scale is transferred to the macroscopic diffusion equation.

Another important remark is that if we have $\epsilon_{1,2}=O(\delta)$ or smaller the above analysis can be carried out with no essential difference. The only difference is that to $O(1)$ terms the quantity $\epsilon_1 U_{0\tau}$, since it is of $O(\delta)$ or smaller, is not included in equation (15). Therefore we get the equation $\nabla_y^2 U_0+\nabla_z^2 U_2=0$ in place of equation (15) and finally the equation $U_{yy}=\frac{1}{\gamma_u\phi_g}g(W)UW^2(1+\beta_1 U)\frac{L(y,\tau)}{A(y,\tau)}$ instead of (21a). The same applies for the water concentration W, in equation (21d) when $\epsilon_2=O(\delta)$ or smaller.

Next in order to simplify the analysis as well as the numerical treatment of the problem we proceed with a change in time variable in the equations for the moving boundary.

In the equation for $S=S(y,z_1,\tau)$, we set

$$\frac{\partial S}{\partial \tau}=\frac{\partial S}{\partial \sigma}\frac{\partial \sigma}{\partial \tau},$$

for σ a new time variable. Thus we obtain

$$-\tfrac{\partial S}{\partial \sigma}\tfrac{\partial \sigma}{\partial \tau}=g\left[W(y,\tau)\right]U(y,\tau)W^2(y,\tau)\sqrt{1+\left(\tfrac{\partial S}{\partial z_1}\right)^2},$$

$$S(y,z_1,0)=S_a(z_1),\quad \tfrac{\partial S}{\partial z_1}(y,0,\tau)=0.$$

We simplify the problem by setting $\frac{\partial \sigma}{\partial \tau}=g\left[W(y,\tau)\right]U(y,\tau)W^2(y,\tau)$ or

$$\sigma=\sigma(\tau)=\int_0^\tau g\left[W(y,\tau')\right]U(y,\tau')W^2(y,\tau')d\tau'.$$

Therefore we obtain a form of the Eikonal equation for $S=S(z_1,\sigma)$,

$$-\frac{\partial S}{\partial \sigma}=\sqrt{1+\left(\frac{\partial S}{\partial z_1}\right)^2},\quad 0<z_1<1,\quad \sigma\geq 0, \tag{22a}$$

$$S(z_1,0)=S_a(z_1),\quad S_{z_1}(0,\sigma)=0. \tag{22b}$$

In the following we present some cases that the above Eikonal equation attains analytical solutions (see [18]). In these cases the system of equations for U and W

take the form of non-local problem. Also for convenience in the following we will use the notation $R(y,\tau) := g\left[W(y,\tau)\right]U(y,\tau)W^2(y,\tau)$.

Sandpile solutions.

Square Segment. We consider the case that the calcium carbonate segment is of a square form, of side say $2L_0$, contained in a square cell with side of length 2. The length of the square side $2L_0$ should be such that $\frac{4-(2L_0)^2}{4} = \phi_c$, and therefore $L_0 = \sqrt{1-\phi_c}$. This corresponds to the following equation.

$$\begin{gathered} -\tfrac{\partial S}{\partial \sigma} = \sqrt{1+\left(\tfrac{\partial S}{\partial z_1}\right)^2}, \quad 0<z_1<1, \quad \sigma \geq 0, \\ S(z_1,0) = L_0, \quad \tfrac{\partial S}{\partial z_1}(0,\sigma) = 0. \end{gathered}$$

The solution of the equation is $S(z_1,\sigma) = L_0 - \sigma$ for $0 \leq z_1 \leq L_0 - \sigma$, or

$$S(y,z_1,\tau) = L_0 - \int_0^\tau R(y,\tau')\,d\tau'.$$

Then the source term in the equation for U, (21a), has the form

$$F_u(U,W) = -\frac{1}{\gamma_u \phi_g} R(y,\tau)\left(1+\beta_1 U(y,\tau)\right) \frac{8\left[L_0 - \int_0^\tau R(y,\tau')d\tau'\right]}{\left[4 - 4\left(L_0 - \int_0^\tau R(y,\tau')d\tau'\right)^2\right]}. \tag{23}$$

The source term for W in equation (21d), similarly is

$$F_w(U,W) := -\frac{1}{\gamma_w \phi_g} R(y,\tau)\left(2+\beta_2 W(y,\tau)\right) \frac{8\left[L_0 - \int_0^\tau R(y,\tau')d\tau'\right]}{\left[4 - 4\left(L_0 - \int_0^\tau R(y,\tau')d\tau'\right)^2\right]}.$$

Cyclical Segment. In that case we assume that initially in a square cell we have a circular cement segment of radius R_0 such that $\frac{4-\pi R_0^2}{4} = \phi_c$, or $R_0 = 2\left(\frac{1-\phi_c}{\pi}\right)^{\frac{1}{2}}$. The Eikonal equation is of the form

$$\begin{gathered} -\tfrac{\partial S}{\partial \sigma} = \sqrt{1+\left(\tfrac{\partial S}{\partial z_1}\right)^2}, \quad 0<z_1<1, \quad \sigma \geq 0, \\ S(z_1,0) = \sqrt{R_0^2 - z_1^2}, \quad 0 \leq z_1 \leq 1, \quad S_{z_1}(0,\sigma) = 0, \quad \sigma \geq 0. \end{gathered}$$

with solution

$$S(y,z_1,\tau) = \left[\left(R_0 - \int_0^\tau R(y,\tau')\,d\tau'\right)^2 - z_1^2\right]^{\frac{1}{2}},$$

for $z_1 < R_0 - \sigma = R_0 - \int_0^\tau R(y,\tau')\,d\tau'$. The source term in the equation for U (for W this can be obtained the same way as before) is

$$F_u(U,W) = -\frac{1}{\gamma_u \phi_g} R(y,\tau)(1+\beta_1 U(y,\tau)) \frac{2\pi\left[R_0 - \int_0^\tau R(y,\tau')\,d\tau'\right]}{\left[4 - \pi\left(R_0 - \int_0^\tau R(y,\tau')\,d\tau'\right)^2\right]}, \tag{24}$$

Cubic Segment. In case that we have a three-dimensional cell, that is a cubic cell, of edge 2 we take $z = (z_1, z_2, z_3) \in \Omega = [-1, 1]^3$. Also we assume that $S(z_1, z_2, 0) = L_0$, $0 \leq z_1 \leq 1$, $0 \leq z_2 \leq 1$. The solution of the Eikonal equation (its three-dimensional version), in this case is $S(z_1, z_2, \sigma) = L_0 - \sigma$, $0 \leq z_1 \leq \sigma$, $0 \leq z_2 \leq \sigma$. Thus

$$F_u(U,W) = -\frac{1}{\gamma_u \phi_g} R(y,\tau)\left(1+\beta_1 U(y,\tau)\right) \frac{3\left[L_0 - \int_0^\tau R(y,\tau')\,d\tau'\right]^2}{\left[1 - \left(L_0 - \int_0^\tau R(y,\tau')\,d\tau'\right)^3\right]}, \tag{25}$$

Spherical Segment. For a spherical initial surface of radius R_0 inside Ω, we have that $\frac{\left(8-\frac{4}{3}\pi R_0^3\right)}{8} = \phi_c$, or $R_0 = \left((1-\phi_c)\frac{6}{\pi}\right)^{\frac{1}{3}}$. The solution for S is $S(z_1, z_2, \sigma) = \left((R_0^2 - \sigma)^2 - z_1^2 - z_2^2\right)^{\frac{1}{2}}$ and

$$F_u(U,W) = -\frac{1}{\gamma_u \phi_g} R(y,\tau)\left(1+\beta_1 U(y,\tau)\right) \frac{4\pi\left(R_0 - \int_0^\tau R(y,\tau')\,d\tau'\right)^2}{8\left[1 - \frac{4}{3}\pi\left(R_0 - \int_0^\tau R(y,\tau')d\tau'\right)^3\right]}. \tag{26}$$

In each of the above cases it is straight forward to get the expressions for F_w by substituting the term $\left(2+\beta_2 W(y,\tau)\right)/\gamma_w$ in place of $\left(1+\beta_1 U(y,\tau)\right)/\gamma_u$ in the corresponding expressions for F_u.

3. Numerical solution.

The numerical solution of the problem can be given, by applying the methodology of [18], as a two stages process. Initially we need to solve the Eikonal equation (22) accounting for the microscopic geometry of the problem and for the cases that we cannot have an analytical solution of it. Next we use this solution to evaluate the source terms in the field equations for U and W and then solve the resulting problem for the macroscale.

Eikonal equation. For the solution of the former problem, i.e. the Eikonal equation (22a) and (22b) and due to its hyperbolic nature, we use a standard upwind scheme ([16]).

Let T_σ being the final time of the simulation. We take the grid $[0,1] \times [0, T_\sigma]$ with $M_\sigma + 1$ points $z_{1j} = j\delta z_1$ in $[0,1]$, for δz_1 being the spatial step for $j = 0, 1, 2, \ldots, M_\sigma$. Similarly in the interval $[0, T_\sigma]$, we take N_σ time steps of size $\delta\sigma$ for $N_\sigma = \left[\frac{T_\sigma}{\delta_\sigma}\right]$ and $\sigma_\ell = \ell\delta\sigma$, $\ell = 1, 2, \ldots, N_\sigma$.

We denote with S_j^ℓ the approximation of $S(z_{1j}, \sigma_\ell)$ and we have

$$S_j^{\ell+1} = S_j^\ell - \delta\sigma\left[1 + \left(\frac{S_j^\ell - S_{j-1}^\ell}{\delta z_1}\right)^2\right]^{\frac{1}{2}}, \quad j = 2, 3, \ldots, M_\sigma, \tag{27}$$
$$S_1^{\ell+1} = S_1^\ell - \delta\sigma, \quad \text{for} \quad j = 1,$$

and $\ell = 2, \ldots, N_\sigma$, while $S_j^1 = S_a(z_{1j})$.

In the case that we have a three-dimensional microstructure and therefore a cubic cell a three-dimensional version of the Eikonal equation has to be solved numerically. In this case the above numerical scheme can be appropriately modified and used in a straight forward way (see [18]).

Evaluation of A and L. Given the approximation of S, S_ℓ^j we are able to calculate the quantities L and A in the source term $F(U,W)$ ($F = F_u$ or F_w depending the case) at each time step. Namely $L = L(S^\ell) = L(\sigma_\ell)$ and $A(S^\ell) = A(\sigma_\ell)$, for $S^\ell = \left(S_1^\ell, S_2^\ell, \ldots, S_{M_\sigma}^\ell\right)$.

We compute the integrals $I_L(S^\ell) \simeq \int_{S^\ell} S(z_1, \sigma_\ell)dz_1$ and $I_A(S^\ell) \simeq \int_0^1 S(z_1, \sigma_\ell)dz_1$ which are the approximations of the quantities $L(S^\ell)$ and $A(S^\ell)$ respectively e.g. via the Simpson's rule.

At this point we need also a grid for the macroscopic domain $[0, T] \times [0, 1]$. We take for $0 \leq \tau \leq T$, $\tau_i = i\delta\tau$, $\delta\tau = \left[\frac{T}{N}\right]$ and for N the time steps. Also for $0 \leq y \leq 1$ we take $M + 1$ points $y_j = j\delta y$, $j = 0, 1, \ldots, M$ for δy the spatial step.

Next the quantities $A(y_j, \tau_i) = A(\sigma_\ell)$ and $L(y_j, \tau_i) = L(\sigma_\ell)$ for some σ_ℓ are needed for evaluating the numerical solution of U and W at each point (y_j, τ_i).

In order to find the index ℓ of σ_ℓ that corresponds to the point (y_j, τ_i) we need to approximate the integral $I_{\tau_i} \simeq \int_0^{\tau_i} R(y, \tau')d\tau'$. Then for some ℓ we have $\sigma_\ell \simeq I_{\tau_i}$. The index ℓ is the one that minimizes the quantity $(\sigma_\ell - I_{\tau_i})$. Thus for this specific ℓ we get $A(y_j, \tau_i) = I_A(\sigma_\ell)$ and $L(y_j, \tau_i) = I_L(\sigma_\ell)$.

Field equations. Recall that we have applied a discetization in the domain $[0, T] \times [0, 1]$. We use a finite element approach. Let Φ_j, $j = 0, \ldots, M$ denote the standard linear B - splines on the interval [0, 1], defined with respect to the partition considered.

$$\Phi_j = \begin{cases} \frac{y - y_{j-1}}{\delta y}, & y_{j-1} \leq y \leq y_j, \\ \frac{y_{j+1} - y}{\delta y}, & y_j \leq y \leq y_{j+1}, \\ 0, & \text{elsewhere in} \quad [0,\ 1], \end{cases} \tag{28}$$

for $j = 0, 1, 2, \ldots, M$.

We then set $U(y, \tau) = \sum_{j=0}^M a_{u_j}(\tau)\Phi_j(y)$, $W(y, \tau) = \sum_{j=0}^M a_{w_j}(\tau)\Phi_j(y)$, $\tau \geq 0$, $0 \leq y \leq 1$.

The standard Galerkin method results in a system of equations for the a_u's and a_w's. Namely for $a = a_u$ or a_w and $\epsilon = \epsilon_1$ or ϵ_2 respectively. Recall also that the source term denoted by F, with $F = F_u$ or F_w, has the form $(1+\beta_1 U)/\gamma_u\phi_g \times RL/A$ in the equation for U and $(2 + \beta_2 W)/\gamma_w\phi_g \times RL/A$ in the equation for W.

$$\begin{aligned} \epsilon \sum_{j=0}^M \dot{a}(\tau) \left\langle \Phi_j(y)\, \Phi_i(y) \right\rangle &= -\sum_{j=0}^M a(\tau) \left\langle \Phi_j'(y)\, \Phi_i'(y) \right\rangle \\ &+ \left\langle F\left(\sum_{j=0}^M a_{u_j}(\tau)\Phi_j(y), \sum_{j=0}^M a_{w_j}(\tau)\Phi_j(y) \right) \Phi_i(y) \right\rangle, \end{aligned} \tag{29}$$

where $\langle f, g\rangle := \int_0^1 f(y)g(y)dy$ and $i = 1, 2, \ldots, M$. Setting $a_u = [a_{u_1}, a_{u_2}, \ldots, a_{u_M}]^T$ $a_w = [a_{w_1}, a_{w_2}, \ldots, a_{w_M}]^T$ The system of equations for the a's takes the form

$$\begin{aligned} A\dot{a}_u(\tau) &= -Ba_u(\tau) + b_u(\tau), \\ A\dot{a}_w(\tau) &= -Ba_w(\tau) + b_w(\tau), \end{aligned}$$

The matrices A and B obtain the standard form in this case (e.g. see [17], [18]) and $b_u = b_u(a_u, a_w)$, $b_w = b_w(a_u, a_w)$ are the arrays coming from the last term in equation (29).

We then apply a three time step approximation, increasing the range of stability of the method compared with the standard two time step approximation, by taking, e.g. in the equation for a_u, $\dot{a}_u(\tau_n) \simeq \frac{a_u^{n+1} - a_u^{n-1}}{2\delta\tau}$. Hence the resulting scheme has the form

$$a_u^{n+1} = (A + \delta\tau B)^{-1} \left[(A - \delta\tau B)a_u^{n-1} + 2\delta\tau\, b_u^n \right]. \tag{30}$$

For $n = 2$ we have in place of equation (30) the following

$$a_u^2 = (A + \delta\tau B)^{-1}\left[(A - \delta\tau B)a_u^1 + \delta\tau\, b_u^1\right],$$

for a_u^1 being determined by the initial condition.

In the cases that we have $\epsilon_{1,2} \ll 1$ we can approximate the problem by getting the versions of the equations (21a), (21d) with the time derivatives omitted. Regarding the numerical solution of the problem in this case we may proceed in a similar way as before. In such a case we need to solve at each time step the system

$$Ba_u^n = b_u(a_u^{n-1}, a_w^{n-1}),$$
$$Ba_w^n = b_w(a_u^{n-1}, a_w^{n-1}).$$

3.1. **Numerical simulations.** In Figure 2 we illustrate the approximate solution to the system of equations (21) with the moving boundaries, $y_l(\tau)$ and $y_u(\tau)$, given by the conditions $\max\{\tau : A(y_l(\tau), \tau) = A_a\}$ and $\min\{\tau : A(y_u(\tau), \tau) = 4\}$ respectively. This solution is plotted against time. The area of a single cell is assumed to be 4 while the initial calcium carbonate area is $A_a = A(y, 0) = 4\left[1 - \int_0^1 S_a(z_1)dz_1\right]$. The y axis corresponds to the macroscopic length of the material. The area between y_l and y_u indicates the mushy region. The boundary y_l describes, e.g. thinking of the corrosion of a marble stone, the motion of point C in Figure 1, while in the same context, y_u describes the motion of point B. In the first case in (a) the calcium carbonate segment is taken to be a square of side $2L_0$ and the source term (23) is adapted in the model and in the system of equations (21). In (b) similarly regarding the source term, we have that the initial calcium carbonate area in one cell is of circular shape with radius R_0 and $A_a = 4 - \pi R_0^2$. The source term of equation (24) was used. Finally in (c) A_a is assumed to be determined by a curve of the form $\frac{x^n}{c_1^n} + \frac{y^n}{c_2^n} = 1$ (Lamé curve) for $n = 6$ and $c_1 = 1$, containing the calcium carbonate. In addition in (d) a simulation has be done for the case that $A_a = A(y, 0) = 4\int_0^1 S_a(z_1)dz_1$ where we have the inverse consideration, i.e. when calcium carbonate is surrounding the gypsum - void area and A_a is the area inside the square cell and outside the curve of the form $\frac{x^n}{c_1^n} + \frac{y^n}{c_2^n} = 1$, again for $n = 6$ and $c_1 = 1$. In the latter case the boundary Γ_c is expanding and we need an inverse sign in equation (22a) and thus we solve in place of it the equation $\frac{\partial S}{\partial \sigma} = \sqrt{1 + \left(\frac{\partial S}{\partial z_1}\right)^2}$. Finally L_0, R_0 and c_2 are evaluated so that $(4 - A_a)/4 = \phi_c$.

Also for a cubic cell (three-dimensional microstructure) we have the boundaries indicated by (A) when the calcium carbonate inside the cell has the form of a cube and (B) when it has the form of a sphere. For the latter simulations equations (25) and (26) was used respectively. We can notice that for the three-dimensional microgeometries, i.e. the case of the cube and the sphere, we have a shift to the left for the boundaries and thus slower corrosion, compared with the two-dimensional cases, i.e. the case of the square and the cycle.

The values of the parameters used in these simulations are for $M = 31$, $T = 1$, $\epsilon_1 = \epsilon_2 = 1$, $\gamma_u = \gamma_w = 10$, $\phi_c = 0.05$, $\phi_g = 0.3$, $w_l = 0.25$, $w_u = 0.75$, $\delta\tau = .8 \cdot \delta y^2$, $M_\sigma = 41$, $\delta\sigma = .1 \cdot \delta z_1$, $T_\sigma = 1$.

In Figure 3, the system of equations (21) is solved numerically again but for the case that $\epsilon_1, \epsilon_2 \ll 1$. In this case the diffusion is faster and therefore the corrosion of the material of length l is faster. Corrosion starts instantly and there is not visible difference for the boundaries y_l. The form of the boundary of the calcium

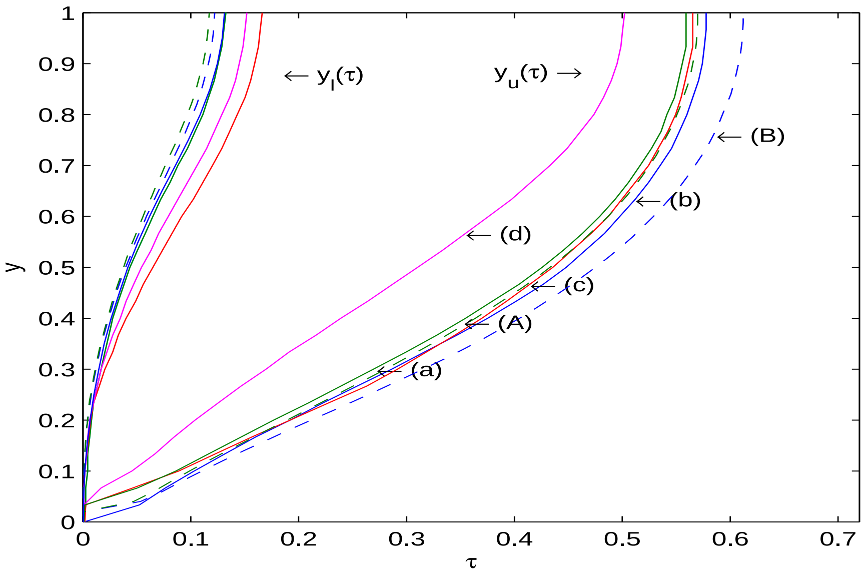

FIGURE 2. *Moving boundaries, indicating when the corrosion starts (y_l) and when is complete (y_u) for a square cell and in the cases that we have an initial calcium carbonate element in the form of (a) a square, (b) a cycle, and (c) a Lamé curve. In the case that calcium carbonate is surrounded by the cell boundary and a Lamé curve we obtain (d). For a cubic cell similarly when the calcium carbonate element has the form of a cube we obtain the boundaries (A) and when this is a sphere we obtain the boundaries (B), denoted with dotted lines.*

carbonate inside a single cell is a factor that reflects on the speed of the corrosion as it is apparent in Figure 3.

The values of the parameters used in these simulations are for $M = 15$, $T = 0.3$, $\gamma_u = \gamma_w = 10$, $\phi_c = 0.05$, $\phi_g = 0.3$, $\delta\tau = .1 \cdot \delta y^2$, $M_\sigma = 101$, $\delta\sigma = .1 \cdot \delta z_1$, $T_\sigma = 1$.

In addition by taking some typical values as those in [4], we have for $D_s = 0.15\,\mathrm{cm}^2/\mathrm{sec}$, $D_w = 0.2178, \mathrm{cm}^2/\mathrm{sec}$, $\lambda_1 = 14.3 \cdot 10^{-12}\,\mathrm{g/cm}^3$, $\lambda_2 = 17.3 \cdot 10^{-6}\,\mathrm{g/cm}^3$, $C_c = 2.83\,\mathrm{g/cm}^3$, $\phi_c = 0.1$, $\phi_g = 0.3$. Also we take $l = 0.012\,\mathrm{cm}$, $\delta = 10^{-2}$ and k_u is estimated so as to give a speed of reaction $v_0 = (4/3.15) \cdot 10^{-11}\,\mathrm{cm/sec} = 4 \cdot 10^{-6}\,\mathrm{m/year}$. This gives $k_u = 2.47 \cdot 10^{11}\,\mathrm{sec}^{-1}\mathrm{g}^{-3}\mathrm{cm}^9$. For these values we have $\epsilon_1 = 1.01 \cdot 10^{-12}$ $\epsilon_2 = 6.9964 \cdot 10^{-13}$, $\gamma_u = 5.98$, $\gamma_w = 1.2685 \cdot 10^{13}$, $\beta_1 = 5.053 \cdot 10^{-12}$ and $\beta_2 = 6.1131 \cdot 10^{-6}$.

These values indicate that diffusion of water is very fast compared with the reaction progress. Therefore we have $W_{yy} \simeq 0$ for $\epsilon_2, 1/\gamma_w \ll 1$. For a constant concentration at the boundary $y = 0$, $W\phi = 1$ and $(W\phi)_y = 0$, at the point $y = 1$, we get

$$W = \frac{1}{\phi(0,\tau)} \left[1 - \frac{\phi_y(1,\tau)}{\phi(1,\tau) + \phi_y(1,\tau)} y \right]. \tag{31}$$

Also the equation for U, given also that $\beta_1 \ll 1$, takes the form

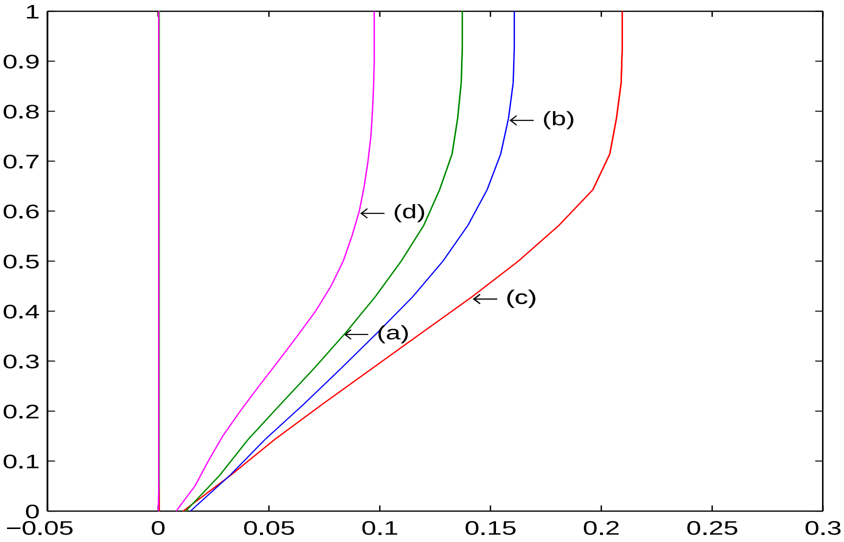

FIGURE 3. *Moving boundaries for the case that* $\epsilon_1, \epsilon_2 \ll 1$*, indicating when the corrosion is complete in the cases of having an initial calcium carbonate element in the form of (a) a square, (b) a cycle and (c) a Lamé curve (for* $n = 6$*). In (d) the initial void of the cell is surrounded by a Lamé curve with calcium carbonate in the exterior of it.*

$$U_{yy} = \frac{1}{\gamma_u \phi_g} g(W) U W^2 \frac{L(y,\tau)}{A(y,\tau)}, \quad 0 < y < 1, \quad \tau \geq 0, \tag{32}$$

with A and L given in the same way by the equations of the system (21). For this case a simulation has been done in Figure 4 where the boundaries y_u and y_l are plotted against time and S_a is taken to be a cycle. We can see that due to the fact that diffusion is fast a layer of thickness $y = 1$ ($x = l = .012\,\text{cm}$), instantly becomes partly corroded, i.e. y_l is placed at the $\tau = 0$ point, while this layer is fully corroded at about 0.17 time units or at about $t = 0.17 \times t_0 = 5,1$ years.

Note that since a few of important factors have not been included in the model, such as the, varying effective diffusivity, the volume expansion of the cell's and consequently the swelling of the corroded layer, the mechanical deformation of the material during the process, the inhomogeneity of the pores inside the calcium carbonate etc., the above results should be interpreted at this stage only qualitative.

4. **Conclusions.**

In this paper a mathematical model for the formation of a mushy region in marble or in general in calcium carbonate stones during corrosion by SO_2, converting calcium carbonate into gypsum, is derived and solved numerically.

This model is a modification of the one presented in [5], [4]. This is adjusted in such a way so as to address the coexistence of corroded and uncorroded parts of the material in a volume element of it. By following the method of averaging as this is prescribed in [17], [18] a system of reaction diffusion equations is derived describing

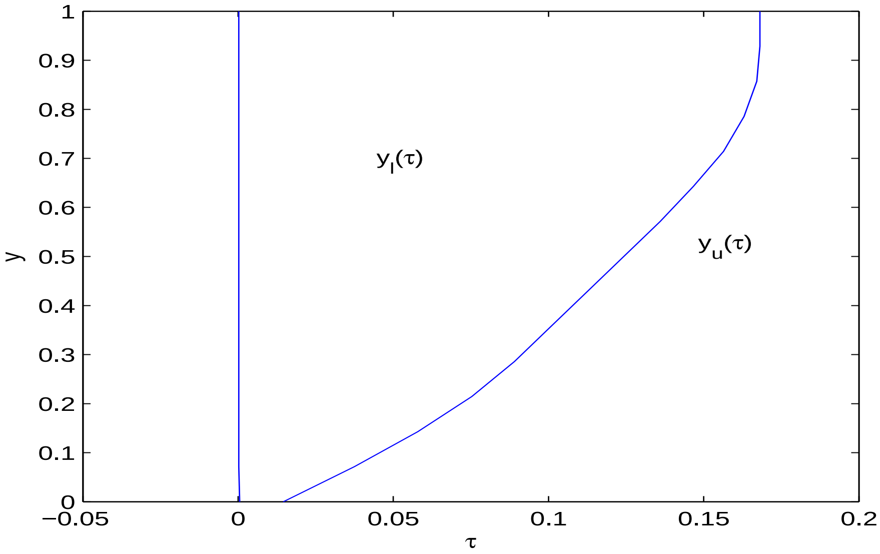

FIGURE 4. *A simulation of the corrosion process for the case that we have equations* (32) *and* (31) *in place of* (21a) *and* (21d) *in the system* (21)*, for small* ϵ_2 *and* γ_w*.*

the process. In these equation the information about the evolution of the corrosion in the microscopic scale is included by the solution of the Eikonal equation. Such a solution describes the motion of the corrosion front in the microscale as a moving boundary in a volume element of the material.

Note also that in the model setting by allowing diffusion in the whole of the cell, so as to avoid complications in the asymptotics and in the numerical treatment of the problem, by having dependence of the $O(1/\delta)$ terms on the microscale length, we obtain a less realistic picture of the phenomenon but still indicative of how this process evolves. Such a model can serve as an initial stage in the study of sulphation process. Inclusion of the diffusion effect in the model, by allowing flow only in a part of the cell is a very important subject to be studied in the future.

The resulting system is solved numerically considering various cases for the geometry of the material in the microscale. The resulting simulations predict corrosion up to a reasonable range. Although due to the fact that there are important factors of the process that should be added in the model such as changing effective diffusivity, volume expansion, mechanical deformation, inhomogeneity of the microstructure geometry etc. the results should be interpreted qualitative. This work can be further improved by including these factors in the model and make it more realistic and useful in practice. Also the study of the multiscale formal asymptotics presented here in a more rigorous context, in the spirit of works as [6] - [10], would be very interesting aspect improving the validity of the model.

REFERENCES

[1] G. Ali, V. Furuholt, R. Natalini and I. Torcicollo, A mathematical model of sulphite chemical aggression of limestones with high permeability. Part I. Modeling and qualitative analysis, *Transport in Porous Media*, **69** (2007), 109–122.

[2] G. Ali, V. Furuholt, R. Natalini and I. Torcicollo, A mathematical model of sulphite chemical aggression of limestones with high permeability. Part II: Numerical approximation, *Transport in Porous Media*, **69** (2007), 175–188.

[3] D. Aregba-Driollet, F. Diele and R. Natalini, A Mathematical Model for the SO2 Aggression to Calcium Carbonate Stones: Numerical Approximation and Asymptotic Analysis, *SIAM J. APPL. MATH.* , **64** (2004), 1636–1667.

[4] F. Clareli, A. Fasano and R. Natalini, Mathematics and monument conservation: Free boundary models of marble sulfation, *SIAM Journal on Applied Mathematics*, **69** (2008), 149–168.

[5] A. Fasano and R. Natalini, *Lost Beauties of the Acropolis: What Mathematics Can Say,* SIAM news, 2006.

[6] T. Fatima, *Multiscale Reaction Diffusion Systems Describing Concrete Corrosion: Modelling and Analysis*, Ph.D thesis, Technical University of Eindhoven, 2013.

[7] T. Fatima, N. Arab, E. P. Zemskov and A. Muntean, Homogenization of a reaction - diffusion system modeling sulfate corrosion of concrete in locally periodic perforated domains, *Journal of Engineering Mathematics*, **69** (2011), 261–276.

[8] T. Fatima and A. Muntean, Sulfate attack in sewer pipes: Derivation of a concrete corrosion model via two-scale convergence, *Nonlinear Analysis: Real World Applications*, **15** (2014), 326–344.

[9] T. Fatima, A. Muntean and T. Aiki, Distributed space scales in a semilinear reaction-diffusion system including a parabolic variational inequality: A well-posedness study, *Adv. Math. Sci. Appl.,* **22** (2012), 295–318.

[10] T. Fatima, A. Muntean and M. Ptashnyk, Unfolding-based corrector estimates for a reaction - diffusion system predicting concrete corrosion, *Applicable Analysis*, **91** (2012), 1129–1154.

[11] F. R. Guarguaglini and R. Natalini, Fast reaction limit and large time behavior of solutions to a nonlinear model of sulphation phenomena, *Commun. Partial Differ. Equations*, **32** (2007), 163–189.

[12] F. R. Guarguaglini and R. Natalini, Global existence of solutions to a nonlinear model of sulphation phenomena in calcium carbonate stones, *Nonlinear Analysis: Real World Applications*, **6** (2005), 477–494.

[13] E. J. Hinch, *Perturbation Methods*, Cambridge University Press, 1991.

[14] A. A. Lacey and L. A. Herraiz, Macroscopic models for melting derived from averaging microscopic Stefan problems I: Simple geometries with kinetic undercooling or surface tension, *Euro. Jnl. of Applied Mathematics*, **11** (2002), 153–169.

[15] A. A. Lacey and L. A. Herraiz, Macroscopic models for melting derived from averaging microscopic Stefan problems II: Effect of varying geometry and composition, *Euro. Jnl. of Applied Mathematics*, **13** (2002), 261–282.

[16] R. J. Leveque, *Finite Volume Methods for Hyperbolic Problems*, Caimbridge University Press, 2002.

[17] C. V. Nikolopoulos, A mushy region in concrete corrosion, *Applied Mathematical Modelling*, **34** (2010), 4012–4030.

[18] C. V. Nikolopoulos, Macroscopic models for a mushy region in concrete corrosion, *Journal of Engineering Mathematics*, 2014, DOI 10.1007/s10665-014-9743-0.

[19] J. L. Schnoor, *Enviromental Modeling, Fate and transport of pollutants in water, air, and soil*, John Willey and Sons, Inc., 1996.

Received March 2014; revised September 2014.

E-mail address: `cnikolo@aegean.gr`